

Long-term optical and X-ray observations of the old novae DI Lacertae and V841 Ophiuchi¹

D. W. Hoard², Paula Szkody³, R. K. Honeycutt⁴, Jeff Robertson⁵, Vandana Desai³,
and T. Hillwig⁴

ABSTRACT

We present an analysis of ground-based optical photometry and spectroscopy, and *Rossi X-ray Timing Explorer* X-ray observations of the old novae DI Lacertae and V841 Ophiuchi. Our optical photometry data (obtained with the automated photometry telescope RoboScope) comprise an almost decade-long light curve for each star, while the contemporaneous spectroscopy and X-ray observations repeatedly sampled each nova during separate intervals of ≈ 45 –55 d in length. The long-term optical light curves of both novae reveal quasiperiodic variability on typical time scales of ~ 30 –50 d with amplitudes of $\Delta V \sim 0.4$ –0.8 mag. V841 Oph also displays a long-term, sinusoidal modulation of its optical light on a time scale of 3.5–5 yr. The optical spectra of these novae display quite different characteristics from each other, with DI Lac showing narrow Balmer emission cores situated in broad absorption troughs while V841 Oph exhibits strong single-peaked Balmer, He I and He II emission lines. We find little change between spectra obtained during different optical brightness states. The X-ray count rates for both novae were very low ($\lesssim 1.5$ ct s^{-1}) and there was no reliable correlation between X-ray and optical brightness. The combined X-ray spectrum of DI Lac is best fit by a bremsstrahlung emission model (with $kT \sim 4$ keV and $N_H < 1.8 \times 10^{22}$ cm^{-2}); the X-ray spectrum of V841 Oph is too weak to allow model fitting. We discuss the possible origin of variability in these old novae in terms of magnetic activity on the secondary star, dwarf nova type disk instabilities, and the “hibernation” scenario for cataclysmic variable stars.

Accepted by PASP on 28 August 2000 for the December 2000 issue.

Subject headings: accretion, accretion disks — novae, cataclysmic variables — stars: individual (DI Lacertae, V841 Ophiuchi)

¹Based on observations with the Apache Point Observatory 3.5-m telescope which is owned and operated by the Astrophysical Research Consortium, and on observations with the WIYN Observatory 3.5-m telescope which is jointly operated by the University of Wisconsin, Indiana University, Yale University, and the National Optical Astronomy Observatories.

²Cerro Tololo Inter-American Observatory, Casilla 603, La Serena, Chile, dhoard@noao.edu

³Department of Astronomy, University of Washington, Box 351580, Seattle, WA 98195-1580

⁴Astronomy Department, Indiana University, Swain Hall West 319, Bloomington, IN 47505

⁵Department of Physical Sciences, Arkansas Technical University, Russellville, AR 72801-2222

1. Introduction

Cataclysmic variables (CVs) are semi-detached interacting binary stars composed of a white dwarf (WD) primary star and a low mass ($\lesssim 0.5M_\odot$) main sequence secondary star, with typical orbital periods of $\lesssim 1$ d. The Roche-lobe-filling secondary star loses mass through the inner Lagrangian point into an accretion disk formed around the WD (for non-magnetic CVs). Classical novae are a subclass of CV in which a thermonuclear runaway is triggered in a reservoir of matter that has been gradually accreted onto the WD. The resultant outburst produces a peak brightness increase of ≈ 6 –15 mag, and releases 10^{44} – 10^{46} erg (see review

in Warner 1995, ch. 5).

The outbursts of novae are often well-observed, and the long term behavior of many dwarf novae and novalike CVs is monitored by the American Association of Variable Star Observers. However, there have been few programs for monitoring the variability of novae at quiescence. One such program, using an automated telescope called RoboScope (see §2.1), has monitored 22 old novae and 42 novalikes, most of them for over 9 years now. RoboScope has found several kinds of unusual photometric behavior. About one-third of the old novae have shown quasi-periodic variability for a year or two, interspersed with stable light curves. These variations do not appear stochastic as they repeat at similar periods when they reappear. Preliminary analysis of RoboScope light curves spanning several years for the old nova DI Lacertae suggested brightness oscillations on a time scale of ≈ 35 d (Honeycutt et al. 1995), while the old nova V841 Ophiuchi also displayed prominent variability (Honeycutt et al. 1994). In order to determine if these oscillations could be related to a disk instability mechanism (as operates in dwarf novae) or to mass transfer or magnetic effects on the secondary star, we attempted a detailed study of DI Lac and V841 Oph, which are among the most active and brightest of the systems showing the oscillations.

DI Lac (= Nova Lac 1910) was a moderately fast nova that reached a maximum brightness of $m_V(\text{max}) = 4.3$ mag during its outburst. V841 Oph (= Nova Oph 1848) was a slow nova that reached a similar brightness, $m_V(\text{max}) = 4.2$ mag (Kukarkin et al. 1971). The reddening for both objects has been measured from *International Ultraviolet Explorer* (*IUE*) ultraviolet and ground-based optical spectra. The range for DI Lac is $E(B - V) = 0.15\text{--}0.41$ (Bruch 1984; Cassatella & Gonzalez-Riestra 1990), while for V841 Oph it is $E(B - V) = 0.30\text{--}0.58$ (Bruch 1984; Cassatella & Gonzalez-Riestra 1990; Weight et al. 1994; Verbunt et al. 1997). Nova shells were not detected in $H\alpha$ for either CV (Cohen 1985). In X-rays, DI Lac was undetected in the *ROSAT* PSPC All Sky Survey, with a 2σ upper limit of 0.013 cts s^{-1} in the 11–201 channel (0.1–2.0 keV) energy range during 299 s total exposure time, while V841 Oph was a marginal detection with 0.017 ± 0.007 cts s^{-1} in the “hard” 0.9–2.0 keV *ROSAT* energy range

(0 ± 0.025 cts s^{-1} in the full *ROSAT* energy range) during 402 s total exposure time (Verbunt et al. 1997).

We report here on the results of ground-based optical photometry and spectroscopy, and *Rossi X-ray Timing Explorer* (*RXTE*) X-ray observations of DI Lac and V841 Oph. The optical photometry comprises an almost decade-long light curve for each star, while the contemporaneous spectroscopy and X-ray observation repeatedly sampled each nova during separate intervals of $\approx 45\text{--}55$ d in length.

2. Observations and Analysis

Our long-term optical photometry of DI Lac and V841 Oph was accomplished from 1990–1998, while the spectroscopic and X-ray observations took place in 1997. These observations are summarized in Tables 1 and 2, and are discussed in detail below.

2.1. Optical Photometry

Our optical photometry data were acquired by RoboScope, a 41-cm telescope in Indiana equipped for automated differential CCD stellar photometry (Honeycutt & Turner 1992). All observatory operations (including data reductions) are accomplished as fully unattended and unsupervised tasks, which makes practical the acquisition of long homogeneous data streams. Typically, RoboScope obtains one or two 4-min exposures per clear night for each of ~ 140 program stars. The data are reduced using the method of incomplete ensemble photometry (Honeycutt 1992). For DI Lac, 85 ensemble stars were used in 987 exposures over 9 observing seasons from 1990 November to 1998 November. For V841 Oph, 24 ensemble stars were used in 611 exposures over 8 observing seasons from 1991 May to 1998 September. The zero-points of the differential light curves were established using secondary standard stars from Henden & Honeycutt (1995, 1997). Six such secondary standards were used for V841 Oph, while 13 were employed for DI Lac. Typical 1σ uncertainties in the calibrated magnitudes are on the order of 0.01–0.05 mag. Over the entire multiyear range of the RoboScope light curves, the mean magnitudes were $V \approx 14.55$ for DI Lac and $V \approx 13.6$ for V841 Oph, with full ranges of variability of $\Delta V \approx 0.9$

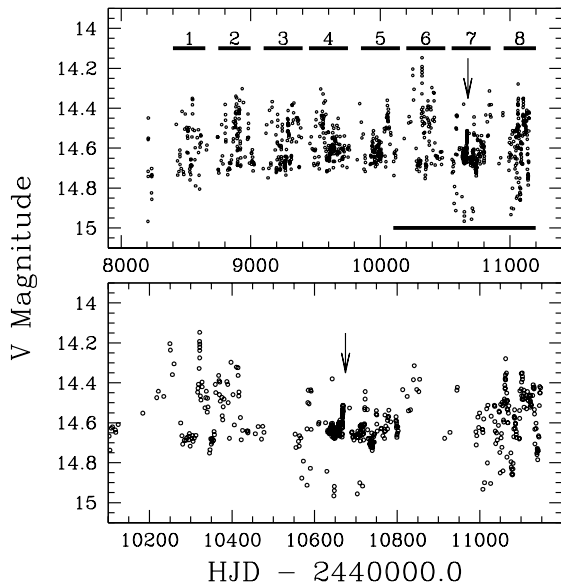


Fig. 1.— The optical (V) light curve of DI Lac from RoboScope. The top panel shows the entire light curve, while the bottom panel shows the region around the $RXTE$ observations. The midpoint time of the $RXTE$ observations is marked with an arrow. The horizontal bars above the data in the top panel show the eight observing seasons (the short initial observing season around HJD 2448200 is not marked), while the bar below the data shows the range of HJD displayed in the bottom panel.

mag and $\Delta V \approx 1$ mag, respectively. The RoboScope light curves of DI Lac and V841 Oph are shown in Figures 1 and 2.

With only limited excursions to anomalously fainter magnitudes, the typical minimum magnitude of ≈ 14.7 for DI Lac has a sharp boundary at any given epoch. However, the minimum brightness displays a slight, apparently linear, trend towards increasing brightness over the 8 years of RoboScope observation. If we ignore for the moment the small number of data points that fall below the well-defined low brightness limit seen in the top panel of Figure 1, then the typical minimum brightness of DI Lac changes from $V \approx 14.75$ mag at the beginning of the RoboScope coverage, to $V \approx 14.67$ mag at the end. This corresponds

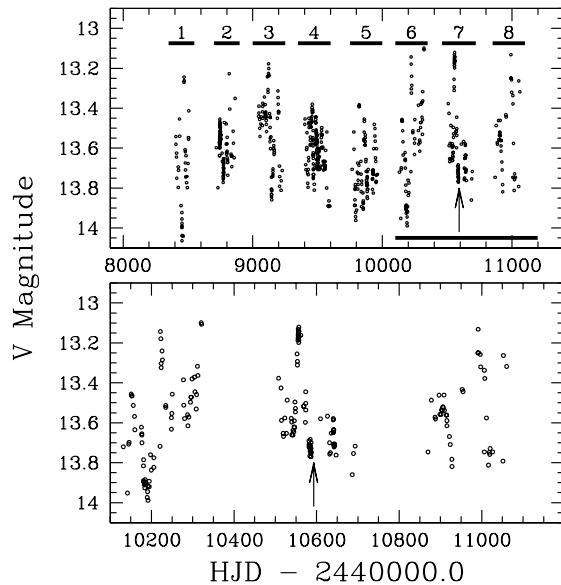


Fig. 2.— As in Figure 1, but for V841 Oph.

to a mean increase of the minimum brightness by $\Delta V \approx -0.01$ mag yr $^{-1}$. The maximum brightness of DI Lac is much less uniform, and it is difficult to determine if the maximum brightness behaves in the same manner as the minimum brightness. A linear fit to the complete DI Lac light curve (with each data point weighted by the inverse square of its 1σ uncertainty) gives the rate of change of the mean magnitude as $< +0.001$ mag yr $^{-1}$; that is, the mean brightness of DI Lac is essentially constant. However, if we exclude the 2 excursions to fainter magnitudes at HJD 2450600 and HJD 2451000 (as well as the excursion to brighter magnitudes at HJD 2450300), then the slope of the linear fit changes to $\Delta V = -0.004$ mag yr $^{-1}$; that is, a trend towards increasing mean brightness.

The faint magnitude excursions in the light curve of DI Lac are very similar to the “dips” seen by Honeycutt et al. (1998a) in long-term RoboScope light curves of five old novae and novalike CVs. In the latter systems, the dips were found to often be paired with a preceding or following outburst, although the dips also sometimes occurred as isolated events. Honeycutt et al. (1998a) do not find a clear mechanism (e.g. disk instabilities, truncated disks, mass transfer modulation) that

is responsible for the dips, but conclude that the overall photometric behavior (dips and outbursts) of the novae and novalikes that they studied is likely to be governed by either a combination of disk and mass transfer events, or by mass transfer events alone.

In contrast to the linear trend in the minimum brightness of DI Lac, the minimum brightness of V841 Oph appears to follow an almost sinusoidal trend that completes approximately 1.5–2 cycles during the 7.5 year RoboScope coverage. As seen in the top panel of Figure 2, the minimum brightness of V841 Oph varies from $V \approx 14.5$ mag to $V \approx 13.8$ mag. The maximum brightness of V841 Oph, which ranges from $V \approx 13.1$ mag to $V \approx 13.4$ mag, displays the same behavior; that is, when the minimum brightness at a given epoch is at its faint (bright) level, the maximum brightness is also at its faint (bright) level. We note that the magnitude range spanned by the minimum brightness in V841 Oph is about twice as large as that spanned by the maximum brightness. Although a linear fit to this overall trend is perhaps not the optimum choice, the corresponding rate of mean magnitude change is $\Delta V = +0.010$ mag yr⁻¹. It is possible (but not required by the data!) that the apparently linear trend in the light curve of DI Lac may also be a sinusoid, but with a much longer cycle length than in V841 Oph.

We searched for periodicities in the range 10–100 days in the RoboScope light curve data in two ways: by applying the phase dispersion minimization (PDM) algorithm (Stellingwerf 1978), as well as performing an independent power spectrum analysis using the CLEAN algorithm (Roberts et al. 1987). We performed the period search on both the entire data set for each CV, as well as on the data subsets from individual observing seasons (indicated in Figures 1 and 2). The most prominent period detected in each data set is listed in Table 3 (in several cases, most notably for the combined data sets for each nova, two significant periods are listed). In general, the two period search methods gave equivalent results to within better than 1–4 days. All of the detected time scales appear to correspond to quasiperiodic behavior rather than truly periodic variability such as that resulting from, for example, an eclipsing orbit. The time scales have significant “flexibility” (on the order of 1–5 days for periods $\lesssim 50$ d,

5–20 days for periods $\gtrsim 50$ d) over the multi-year length of the light curves (as shown by substantially broadened dips and peaks in the PDM and CLEAN analyses, respectively). Phase-binned light curves of both CVs folded on the shorter period found for each combined data set are shown in Figure 3. We note that the true amplitude of variation in a given cycle or observing season will be larger than the 0.1–0.2 mag suggested by Figure 3, in which data from many cycles with slightly different amplitudes and periods have been averaged together. Inspection of Figures 1 and 2 shows amplitudes of 0.4–0.8 mag for the full range of variability within each observing season. The long-term sinusoidal trend in the light curve of V841 Oph is also well-fit by a periodicity in the range 1800–1900 d or, with slightly less agreement, 1250–1300 d. (We note that these two period ranges are approximately related by the ratio 3:2, so we are likely seeing an aliasing effect due to the fact that only 1.5–2 cycles of these long periods are contained in the light curves.)

2.2. Optical Spectroscopy

We obtained optical spectra of both CVs using the Double Imaging Spectrograph on the Apache Point Observatory (APO) 3.5-m telescope (Gillespie et al. 1995)⁶ during University of Washington share time. Spectra of DI Lac were obtained in July and August of 1997; spectra of V841 Oph were obtained in May of 1997. The APO spectra have a resolution of $\approx 2\text{\AA}$ and cover simultaneous wavelength ranges of $\approx 4200\text{--}5000\text{\AA}$ and $\approx 5800\text{--}6800\text{\AA}$. The raw spectrum images were reduced in the standard fashion using IRAF. The instrumental response was removed via spectra of standard stars (Massey et al. 1988) obtained on the same nights; however, slit losses due to guiding errors rendered the absolute flux calibration unreliable. Consequently, we have normalized the spectra to a constant continuum level of 1.0.

A representative spectrum of DI Lac is shown in Figure 4. Note the prominent Balmer absorption troughs containing narrow, central emission cores. Our other two APO spectra of DI Lac (not shown) are essentially identical to this one, with the exception that the Balmer emission cores in the August spectrum are somewhat stronger (relative to

⁶also see <http://www.apo.nmsu.edu/>

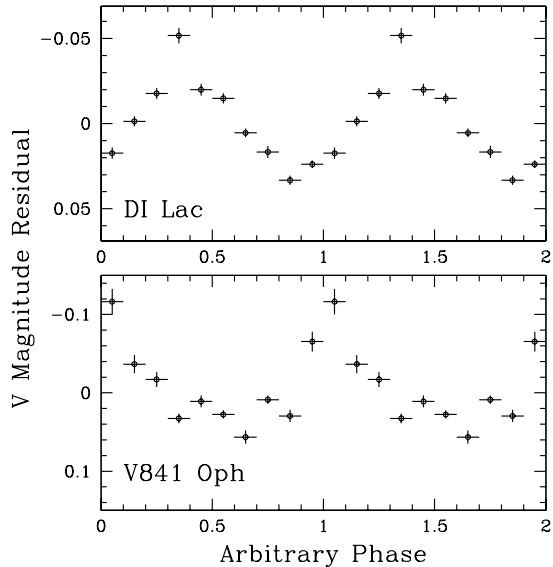


Fig. 3.— The RoboScope light curves of DI Lac (top panel) and V841 Oph (bottom panel) folded on periods of 37 d and 36 d, respectively. A best-fit linear trend was subtracted prior to folding. The data have been averaged into phase bins of width 0.1, and are repeated twice. The horizontal error bars show the width of the phase bins, while the vertical error bars span $\pm 3\sigma_n$, where σ_n is the standard deviation of the mean in each phase bin.

He II) than in the July spectra. The He I $\lambda 4471$ feature (see inset) is present with the same profile shape in all three of our spectra. It is suggestive of the absorption trough with central emission as seen in the Balmer lines. The feature labeled with “?” is likely an instrumental or reduction artifact since its wavelength does not match any identifiable line and it occurs in *all* of our APO spectra (those of V841 Oph included).

Additional optical spectra of both novae were obtained using the Hydra Multi-fiber Positioner + Bench Spectrograph (Barden et al. 1993, 1994) on the WIYN 3.5-m telescope⁷. Spectra of DI Lac were obtained in 1997 September, and spectra of V841 Oph were obtained in 1997 May. The WIYN spectra have a resolution of $\approx 1\text{\AA}$ and cover (usable) wavelength ranges of $\approx 6200\text{--}6800\text{\AA}$ for DI

⁷see <http://www.noao.edu/wiyn/>

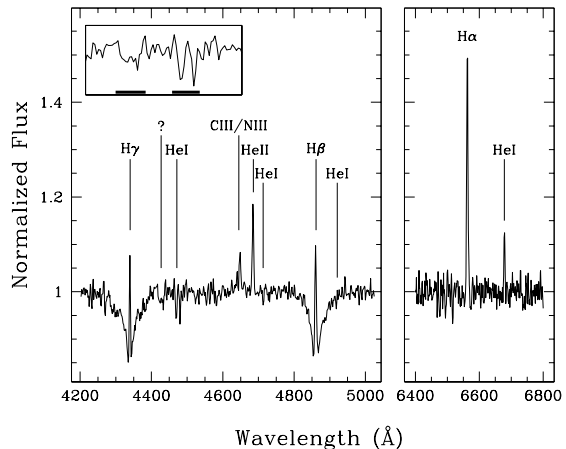


Fig. 4.— Representative optical spectrum of DI Lac from APO on 1997 Jul 25 09:01:47 UT (HJD 2450654.87744). The spectrum has been normalized to a continuum level of 1.0. The wavelengths of prominent line transitions are marked. The box inset in the left panel shows an expanded view of the region from 4390\AA to 4520\AA . The two features highlighted by dark underlines are marked (from left to right) “?” and “HeI” in the full spectrum plot.

Lac and $\approx 4400\text{--}5000\text{\AA}$ for V841 Oph. For the WIYN spectra of DI Lac, no standard star observations were available, so it was not possible to correct for the instrumental response or perform a flux calibration. We do not show these spectra here, but note that they are qualitatively similar to the red APO spectrum shown in Figure 4 – no differences corresponding to the different brightness levels in the RoboScope light curve are apparent. The V841 Oph WIYN data were reduced and calibrated as with the APO spectra. Again, slit losses and, additionally, the presence of cirrus made the absolute flux calibration unreliable, so we have normalized the spectra to a constant continuum level of 1.0. All of the spectra of V841 Oph are shown in Figure 5 (the three WIYN spectra have been averaged together to improve the S/N). There is no indication of the absorption troughs seen in the spectra of DI Lac. Additionally, the C III/N III + He II emission complex appears to be stronger, with broader lines, in V841 Oph than in DI Lac.

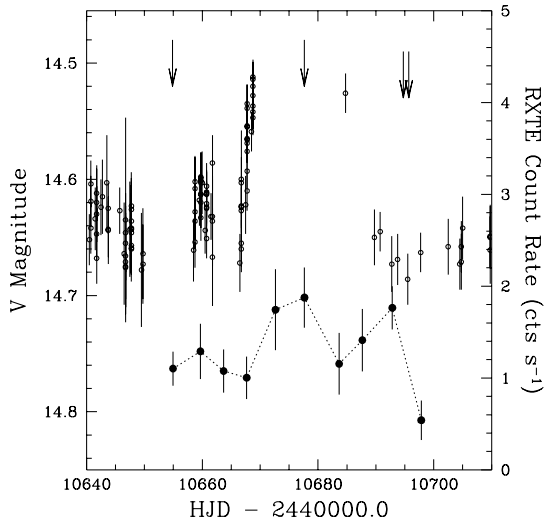


Fig. 6.— The optical (V) light curve of DI Lac from RoboScope (small circles, left axis scale) with the mean $RXTE$ count rate (0–15 keV) at each of the ten epochs of observation (large circles connected by a dotted line, right axis scale). One-sigma error bars are shown on all of the points; the arrows mark the times when optical spectra were obtained. The lowered arrows mark the WIYN spectra; the others are from APO.

Lac and $0.56 \pm 0.73 \text{ ct s}^{-1}$ for V841 Oph. Considering these very low count rates, it is not clear whether or not the variability seen in the X-ray light curves is real.

Additional analysis and model-fitting (DI Lac only) of the X-ray spectra of these novae was performed using the routine XSPEC (v11). Although we extracted the full range of available energy channels in the X-ray spectra, only the range 0–15 keV was used for fitting the models to the DI Lac data. The X-ray spectra for DI Lac and V841 Oph are shown in Figures 8 and 9. The X-ray spectrum of V841 Oph is shown on the same scale as that of DI Lac; the former is clearly much weaker than the latter. We attempted to extract a better spectrum of V841 Oph by using only the data from the four visits with the largest count rates (visits 3, 5, 9, and 11 – see Table 2). Unfortunately, this spectrum was virtually identical to the total combined spectrum (i.e. flat and featureless),

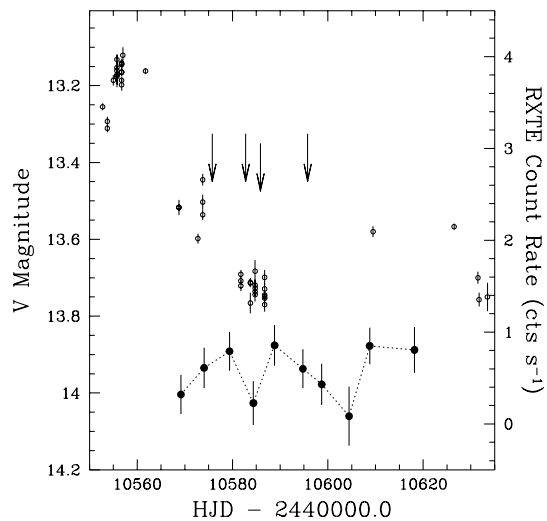


Fig. 7.— As in Figure 6, but for V841 Oph.

with the exception of a small upward offset of the mean count rate, from about $0.02 \text{ cts s}^{-1} \text{ keV}^{-1}$ in the total combined spectrum to about $0.04 \text{ cts s}^{-1} \text{ keV}^{-1}$ in the “high” count rate spectrum. Consequently, no attempt was made to fit a model to the spectrum of V841 Oph.

For DI Lac, we fit three simple models to the X-ray spectrum: (1) blackbody, (2) Raymond-Smith thermal plasma, and (3) bremsstrahlung. Each model was modified by a multiplicative component representing photoelectric (H column) absorption. More complex models were not warranted owing to the small number of counts per energy channel in the data. In all cases, the data were weighted using the XSPEC-recommended scheme appropriate for small count numbers, $W_i = 1 + (N_i + 0.75)^{0.5}$ (Gehrels 1986). The results of these model fits are summarized in the first three rows of Table 4. All of the models produce nearly indistinguishable fits to the observed spectrum. The bremsstrahlung model is formally the best-fitting (with lowest reduced χ^2 and highest null hypothesis probability) and is plotted over the observed spectrum in Figure 8.

All of the models were only able to constrain the hydrogen column density to an upper limit; the values of N_H quoted in the first three rows of Table 4 are the upper ends of the 1-parameter 90%

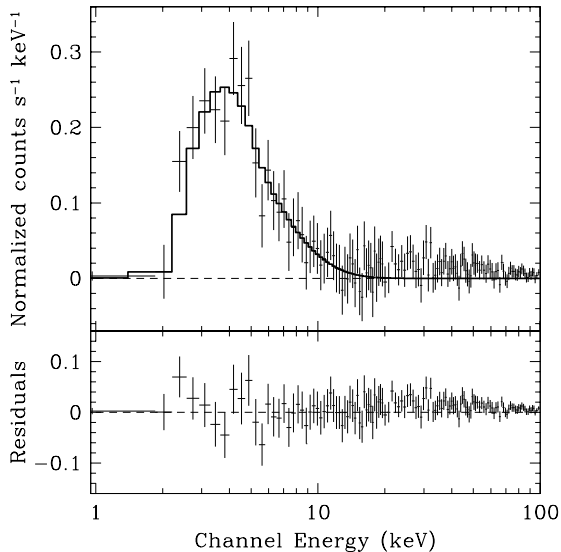


Fig. 8.— Top panel shows the combined X-ray spectrum of DI Lac (crosses) with the best-fitting bremsstrahlung model modified by photoelectric (H column) absorption (solid line). Bottom panel shows the residuals to the model fit.

confidence intervals. We used the relation

$$N_{\text{H}} = E(B - V) \times 5.8 \times 10^{21} \text{cm}^{-2} \text{mag}^{-1}$$

(Bohlin et al. 1978) to estimate values of N_{H} spanning the reddening range given in §1. We then re-fit the models to the X-ray spectrum of DI Lac with only two free parameters: temperature and normalization. The results are listed in the bottom six rows of Table 4. While slightly different from those obtained from the original model fits, they are completely consistent with them. The bremsstrahlung model yields a slightly lower nominal temperature of $kT \approx 4.1\text{--}4.2$ keV (vs. $kT = 4.5$ keV when N_{H} is a free parameter) and is still the best-fitting model for both values of N_{H} .

We note that the uncertainties quoted in Table 4 for kT and C_{norm} are 1-parameter 90% confidence intervals; the interdependent parameter uncertainties will be slightly different. For example, for the bremsstrahlung model (with free N_{H}), the XSPEC routine `steppar`¹⁰ gives a 2-parameter 90%

¹⁰This routine iteratively refits the model to the data while

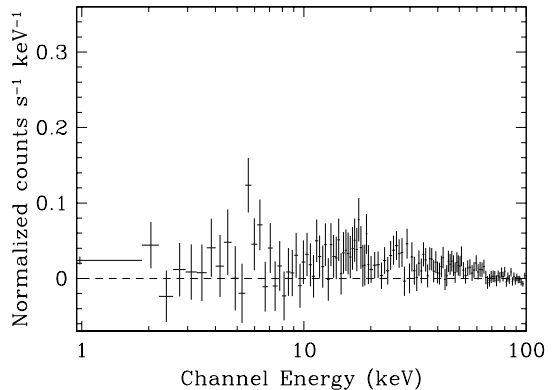


Fig. 9.— The combined X-ray spectrum of V841 Oph on the same scale as the X-ray spectrum of DI Lac shown in Figure 8.

confidence interval of

$$kT = 4.5_{-1.5}^{+1.9} \text{ keV}$$

for kT with respect to N_{H} , and

$$kT = 4.5_{-1.7}^{+1.8} \text{ keV}$$

for kT with respect to C_{norm} .

The X-ray count rates were too low to reliably fit spectrum models to any of the ten individual *RXTE* visits to DI Lac. We constructed “low” and “high” state X-ray spectra by combining the data from visits with the lowest mean count rates (1, 2, 3, 4, 7) and from visits with the highest mean count rates (5, 6, 9) to see if there were any differences between the low and high X-ray brightness states¹¹. Other than an $\approx 1 \text{ cts s}^{-1} \text{ keV}^{-1}$ increase at the peak energy of the high state spectrum, the two spectra are essentially indistinguishable from each other (and from the combined spectrum from all ten visits). We conclude from this that either the spectral energy distribution of the X-ray emitting source in DI Lac does not change as the overall brightness of the X-ray source changes,

stepping the values of selected parameters through a given range and produces a plot in parameter space of the 2-dimensional χ^2 contours.

¹¹Visits 8 and 10 were not used. The former was deemed to be an “intermediate” brightness state, and the latter an anomalously low state.

or that the variability seen in the X-ray light curve of DI Lac is not real (i.e. it is a side-effect of the very low count rates).

3. Discussion

3.1. Optical Photometric Variability

Inspection of the RoboScope light curves of DI Lac and V841 Oph reveals variability on three distinct time scales. First, in the range 10–100 d, quasiperiods with typical lengths of ~ 30 –50 d are present in each of these CVs. Yet, the presence (or lack) of periodic and/or quasiperiodic variability on time scales up to a few hundred days in V841 Oph has been contested in the literature. (To the best of our knowledge, no extensive database of photometric observations of DI Lac has been published prior to this work.) Using 420 archival visual observations of V841 Oph spanning 28 yr, Della Valle & Rosino (1987) quote an average period of 51.5 d with individual cycles ranging from 45 d to 57 d. Shara et al. (1989) observed V841 Oph once per night for 31 nights during a 45 night interval in 1986 using a CCD camera + *B* filter, and found a period of ~ 40 d. All of these values are comparable to the ~ 35 –50 d we found for our complete RoboScope light curve of V841 Oph, as well as to the range of periods found for individual observing seasons in the RoboScope data (see Table 3). On the other hand, Duerbeck (1992) notes the presence of considerable variability in archival light curves of V841 Oph (including some of the same data used by Della Valle & Rosino 1987), but finds no evidence for periodicities up to 200 d.

It is quite interesting that the variability time scales in these two novae are similar to those that characterize dwarf nova outbursts (Warner 1995, ch. 3). Old novae are presumed to have mass transfer rates, \dot{M} , above the threshold level (\dot{M}_{crit}) at which the accretion disk thermal instability mechanism operates in dwarf novae to produce their outbursts (Osaki 1996). However, the hibernation theory of cyclic evolution between CV variability types (Shara 1989, and references therein), predicts that when \dot{M} eventually decreases back into the instability regime some decades after the nova outburst, then dwarf nova outbursts should resume. Both GK Persei (= Nova Per 1901; Bianchini et al. 1986) and V446 Herculis (= Nova Her 1960; Honeycutt et al. 1998b) have displayed dwarf

nova eruptions in their post-nova stages, and similar behavior has been suggested for a number of other old novae, commencing ≈ 50 –200 yr after their outbursts (Livio 1989; Warner 1995, ch. 4). The amplitudes of variability displayed by DI Lac and V841 Oph (see Figures 1 and 2) are smaller than those typically observed for dwarf novae ($\Delta V \sim 2$ –4 mag), but we cannot rule out the possibility of a disk instability mechanism being in operation – after all, it has been 90 years since the nova outburst of DI Lac and over 150 years since that of V841 Oph. Further, the classic thermal instability mechanism is not well-explored for high- \dot{M} disks, and other disk instabilities might operate as well (e.g. Whitehurst 1988; Mineshige 1993; Godon 1998).

The amplitudes of the ~ 30 –50 d oscillations in DI Lac and V841 Oph are similar to those of the spaced stunted outbursts seen in some nova-like CVs (Honeycutt et al. 1998a). One of the suggestions for stunted outbursts made in Honeycutt et al. (1998a) is that they are dwarf nova eruptions seen against a background of brighter light in the system. If that suggestion is correct, then the oscillations reported here (as well as similar 25 d oscillations reported for RW Tri, Honeycutt et al. 1994) may be examples of dwarf nova type outburst behavior at relatively short recurrence times, $T_n \lesssim 50$ d (T_n is typically $\gtrsim 10$ d to hundreds of days – even tens of years in extreme cases – for dwarf novae; Warner 1995, ch. 3). Among the true dwarf novae, the Z Camelopardalis stars have outburst recurrence times of ≈ 10 –30 d, somewhat shorter than the time scales for the oscillations observed in these novae. The Z Cam stars are thought to have high mass transfer rates (near \dot{M}_{crit}). This suggests that if the oscillations observed in novae are analogous to dwarf nova outbursts, then they may be linked to the presence of relatively high mass transfer rates that are, nonetheless, smaller than both \dot{M}_{crit} and \dot{M} in the Z Cam stars.

Second, V841 Oph displays a distinct sinusoidal variation with a best period of 1800–1900 d (4.9–5.2 yr) or a slightly less preferred period of 1250–1300 d (3.4–3.6 yr). DI Lac does not appear to display similar sinusoidal variability, unless it occurs with a much longer period than in V841 Oph. Bianchini (1990) reports a long-term period in V841 Oph of 3.4 yr with mean amplitude of

~ 0.3 mag, which was determined from 420 visual observations spanning 30 yr (essentially the same early- to mid-20th century data utilized by Duerbeck 1992, see below). Richman et al. (1994) re-analyzed the light curves presented by Bianchini (1990) and consider the case for a multi-year periodicity in V841 Oph to be very weak. However, with our RoboScope light curve, sinusoidal variability on comparable multi-year times scales has now been observed in two separate data sets for V841 Oph spanning almost 80 years of observation. While this still does not provide firm evidence of strictly periodic behavior, it certainly points to the presence of a mechanism operating in this CV that modulates its brightness on a characteristic time scale of several years.

Photometric variability in old novae on time scales of several years has generally been attributed to solar-type magnetic cycles on the secondary star that might be able to control the rate of mass loss through the inner Lagrangian point (Bianchini 1990; Applegate 1992). Although Richman et al. (1994) find that no CV studied to date displays strictly periodic behavior over multi-year intervals, they also note that the observed amplitudes (~ 0.2 mag) and “apparent” time scales of variability of 5–40 yr are “plausible consequences from solar-type magnetic cycles.” We note that the shorter time scale (~ 30 –50 d) variability discussed above might also be linked to modulation of \dot{M} due to secondary star magnetic activity. If solar-type magnetic cycles can affect \dot{M} on time scales of years, then starspots induced by the magnetic cycle that migrate under the L_1 point might also affect \dot{M} on shorter time scales, in a manner suggested by Livio & Pringle (1994) to explain the very low brightness states seen in some CVs.

Third, the mean magnitudes of both CVs are changing slowly, at rates measured in a few millimagnitudes (mmag) per year. The mean brightness of DI Lac is increasing by 4 mmag yr^{-1} since 1990. Duerbeck (1992) analyzed a large set of visual, photoelectric, and CCD observations of post-novae available in the literature (see references in Duerbeck 1992). These data cover a large part of the 20th century, from the 1920’s through the 1980’s. Duerbeck (1992) summarizes the long-term behavior of DI Lac as exhibiting a steady decline of 13 ± 1 mmag yr^{-1} in visual observations obtained between 1921 and 1952. Sparse photo-

electric and CCD data from 1953 to 1981 suggest a possible small brightness increase, which is supported by our recent RoboScope observations. For V841 Oph, visual observations from 1919–52 and 1978–91 yield a brightness decline of 7 ± 1 mmag yr^{-1} , while “no definitive brightness decline” (Duerbeck 1992) was found in photoelectric data from 1954 to 1988. Our post-1991 observations of V841 Oph suggest a trend towards decreasing mean brightness comparable to that noted by Duerbeck (1992) in the archival visual observations, although the obvious sinusoidal variation that dominates our light curve at long time scales makes this conclusion somewhat suspect.

In the “classical” hibernation scenario (Shara 1989), novae stay bright for ~ 50 –300 yr following outburst, gradually declining in brightness during this time to a hibernating state characterized by low brightness ($M_V \sim 10$ or fainter) and low mass accretion rate ($\dot{M} \lesssim 10^{-12} M_\odot \text{yr}^{-1}$). However, the photometric record of DI Lac from the 1920’s (a decade after its outburst) to the 1990’s does not show a simple decline in brightness. Instead, the brightness of DI Lac decreased for about four decades after outburst, but then apparently leveled off for several decades. In the last decade (covered in our RoboScope light curve), the brightness of DI Lac has been increasing. It is possible that we are seeing the influence of a mechanism (such as magnetic activity of the secondary star – see above – and/or accretion-induced irradiation of the secondary star) that modulates \dot{M} (and, hence, the brightness) in DI Lac over a long-term cycle (with period on the order of many decades) that obscures the general decline predicted by the hibernation scenario.

3.2. Optical Spectrum Variability

The optical spectra of DI Lac and V841 Oph are quite different, and this can possibly be ascribed to their difference in post-outburst ages. The spectrum of V841 Oph is similar to those of novalike CVs (e.g. Warner 1995, ch. 4) – this suggests that V841 Oph still has a high accretion rate, even ≈ 150 yr after outburst. The narrow emission components in DI Lac are suggestive of emission originating from the irradiated inner face of the secondary star, while the absorption troughs imply the presence of optically thick material in the system. The latter feature could be material

ejected during the outburst of this younger post-nova; the lack of any detected $H\alpha$ emission shell (Cohen 1985) does not preclude the existence of denser, non-emitting circumstellar material. The former feature offers a possible explanation for the gradual brightness increase seen in our RoboScope light curve of DI Lac (discussed in §3.1) if the secondary star is being slowly heated via irradiation and is, in turn, increasing the rate of mass transfer through the L_1 point.

Although the RoboScope coverage is incomplete, we infer from the adjacent data that DI Lac was faint during our July spectra and bright during our August spectrum (see Figure 6). As mentioned in §2.2, the only difference between our July and August spectra is that the emission cores were somewhat stronger in August (bright state) than July (faint state). This is consistent with the hypothesis that these narrow emission features originate on the irradiated face of the secondary star if we make the logical assumption that the irradiation increases when DI Lac is bright. It does not, however, illuminate the exact mechanism producing the irradiation (i.e. whether the “excess” flux in the high state originates near the disk center – presumably due to a disk instability producing increased accretion onto the WD – or in the outer disk – presumably due to an increase in mass transfer through the L_1 point.) If we assume that the spectrum shown in Figure 4 (from July 27 09:01:47 UT) was obtained at an arbitrary orbital phase of 0.0, then the August 17 spectrum was obtained at a relative orbital phase of 0.9 (using $P_{\text{orb}} = 0.543773$ d; Ritter & Kolb 1998). Thus, these two spectra were obtained at similar orbital phases, and we do not expect the difference in the narrow emission component strength to be only due to system orientation.

The RoboScope coverage of V841 Oph during our spectroscopic (and X-ray) observations is more sparse than for DI Lac, but we can infer that the CV was returning to the faint state during our May 07 spectrum, was in its faint state during our May 14 and 17 spectra, and was likely near the bright state during our May 27 spectrum (see Figure 7). (The two elevated brightness points at HJD 2450610 and HJD 2450625 suggest that V841 Oph may have returned to a bright state sometime between the low states bracketing HJD 2450590 and HJD 2450630.) If this is the case, then the

somewhat stronger $H\alpha$ emission of the May 07 and May 27 spectra (see Figure 5) may be linked to the bright state of the CV. As with DI Lac, we calculated relative orbital phases for each of these spectra (using $P_{\text{orb}} = 0.60423$ d; Ritter & Kolb 1998), and obtained $\phi = 0.0, 0.6, 0.75, 0.1$ for May 07, 14, 17, 27, respectively. Unfortunately, this casts some doubt on the link between $H\alpha$ emission strength and brightness state, since both of the bright state spectra (phases 0.0, 0.1) were obtained at different orbital phases than the faint state spectra (phases 0.6, 0.75). So, we cannot rule out the influence of system orientation effects in these spectra.

3.3. X-ray Variability

Unfortunately, because of the weak X-ray emission from these CVs, little can be firmly stated about their X-ray variability. The count rates during visits 5 and 6 to DI Lac, which took place when we infer from the RoboScope light curve that the CV was in a bright state, are slightly elevated compared to the preceding visits. However, visit 7 also occurred during this optical bright state and does not show an elevated count rate. The mean X-ray count rate during each visit to V841 Oph also does not display any strong correlation with the corresponding optical state. The lack of large changes in X-ray flux or spectrum during the optical variations (as usually evident in dwarf novae; e.g. Szkody et al. 1999), argues against a disk instability scenario. Alternatively, this could indicate that the optical brightness is determined by activity in the outer disk only and, therefore, is not reflected in the X-ray behavior; however, the X-ray count rates are too low (and their corresponding error bars too large) to make any firm conclusions.

4. Conclusions

Our long-term optical light curves of the novae DI Lac and V841 Oph obtained with RoboScope reveal quasiperiodic variability with a characteristic time scale of ~ 30 – 50 d in both CVs. In addition, the light curve of V841 Oph displays evidence for sinusoidal variability with a period of 3.5–5 yr. The latter cannot be said to be strictly periodic since our data set covers only ≈ 1.5 cycles; however, when this detection is added to past reports

of multi-year periodicities in V841 Oph that have been reported in the literature, a strong case can be made for the presence of repeating multi-year variability with a preferred time scale in this CV. The most likely origin of such behavior is a solar-type magnetic cycle of the secondary star that modulates the rate of mass transfer through the L_1 point. If this is the case, then the shorter ~ 30 – 50 d quasiperiodic variability in this system might also be related to the magnetic activity on the secondary star; for example, due to starspots that migrate under the L_1 point and temporarily throttle mass transfer. DI Lac does not show evidence for cyclic multi-year variability, unless it occurs with a much longer period than the length of our RoboScope coverage ($\gtrsim 10$ yr). This casts some doubt on the origin of the ~ 30 – 50 d quasiperiodic variability as a facet of the secondary star’s magnetic activity, since both V841 Oph and DI Lac show the ~ 30 – 50 d quasiperiodic behavior, but only V841 Oph displays evidence for a multi-year solar-type magnetic cycle on the secondary star. On the other hand, the ~ 30 – 50 d time scale is very reminiscent of that expected for dwarf nova type behavior (although the amplitude of variability in these novae is smaller than in typical dwarf nova outbursts). This raises the possibility that this variability is caused by a disk instability (either the thermal disk instability that leads to dwarf nova outbursts operating at a low level or some other form of disk instability).

The X-ray spectrum of DI Lac is fit almost equally well by the three models we tried: a simple blackbody, a Raymond-Smith thermal plasma, and bremsstrahlung emission. More complicated models (e.g. involving multiple components, lines, etc.) are unwarranted due to the low X-ray flux. In addition to being the most physically plausible X-ray emission mechanism in a (non-magnetic) CV, the bremsstrahlung model is formally the best-fitting. Our X-ray spectrum model fit parameters ($kT \sim 4$ keV) are consistent with those obtained from *ROSAT* X-ray spectra of a sample of 37 disk-accreting CVs (Richman 1996). Unfortunately, the X-ray count rates in both of these systems were too low for any conclusions to be made about their time-resolved X-ray behavior. X-ray observations sample the innermost disk region, and we would expect to see different time-resolved behavior as the novae go into

their optically bright state if the transition is triggered by a disk instability vs. a change in \dot{M} from the secondary star. Additional time-resolved X-ray observations using the more sensitive *Chandra* and/or *XMM* X-ray satellites may be necessary to illuminate the inner workings of these old novae.

PS, DWH, and VD acknowledge support from NASA grant NAG5-4791. DWH thanks the NOAO librarian Mary Guerrieri for her valuable assistance locating several papers cited herein. This research made use of NASA’s Astrophysics Data System Abstract Service and the SIMBAD database operated by CDS, Strasbourg, France.

REFERENCES

- Applegate, J. H. 1992, *ApJ*, 385, 621
- Barden, S. C., et al. 1993, in *Fibre Optics in Astronomy II*, ASP Conf. Ser. 37, ed. P. M. Gray (San Francisco: Astronomical Society of the Pacific), 185
- Barden, S. C., Armandroff, T., Muller, G., Rudeen, A. C., Lewis, J., Groves, L. 1994, in *Instrumentation in Astronomy VIII*, eds. D. L. Crawford, E. R. Craine, *Proc. SPIE* 2198, 87
- Bianchini, A. 1990, *AJ*, 99, 1941
- Bianchini, A., Sabbadin, F., Favero, G. C., Dalmeri, I. 1986, *A&A*, 160, 367
- Bohlin, R. C., Savage, B. D., Drake, J. F. 1978, *ApJ*, 224, 132
- Bradt, H. V., Rothschild, R. E., Swank, J. H. 1993, *A&AS*, 97, 355
- Bruch, A. 1984, *A&AS*, 56, 441
- Cassatella, A., Gonzalez-Riestra, R. 1990, in *Physics of Classical Novae*, *Proc. IAU Colloq.* 122, eds. A. Cassatella, R. Viotti (Berlin: Springer-Verlag), 115
- Cassatella, A., Selvelli, P. L., Gilmozzi, R., Bianchini, A., Friedjung, M. 1989, in *Accretion Powered Compact Binaries: Proc. of the 11th N. American Workshop on CVs and LMXBs*, ed. C. W. Mauche (New York: Cambridge University Press), 373

- Cohen, J. G. 1985, *ApJ*, 292, 90
- Della Valle, M., Rosino, L. 1987, *IBVS*, 2995
- Duerbeck, H. W. 1992, *MNRAS*, 258, 629
- Feldman, U. 1992, *Physica Scripta*, 46, 202
- Gehrels, N. 1986, *ApJ*, 303, 336
- Gillespie, B., Loewenstein, R. F., York, D. 1995, in *New Observing Modes for the Next Century*, ASP Conf. Ser. 87, eds. T. Boroson, J. Davies, I. Robson (San Francisco: Astronomical Society of the Pacific), 97
- Godon, P. 1998, *ApJ*, 502, 382
- Greenstein, J. L. 1960, in *Stellar Atmospheres*, ed. J. L. Greenstein (Chicago: University of Chicago Press), 676
- Henden, A. A., Honeycutt, R. K. 1995, *PASP*, 107, 324
- Henden, A. A., Honeycutt, R. K. 1997, *PASP*, 109, 441
- Honeycutt, R. K. 1992, *PASP*, 104, 435
- Honeycutt, R. K., Robertson, J. W., Turner, G. W. 1995, in *Cataclysmic Variables*, eds. A. Bianchini, M. della Valle, M. Orio (Dordrecht: Kluwer Academic Publishers), 75
- Honeycutt, R. K., Robertson, J. W., Turner, G. W. 1998a, *AJ*, 115, 2527
- Honeycutt, R. K., Robertson, J. W., Turner, G. W., Henden, A. A. 1998b, *ApJ*, 495, 933
- Honeycutt, R. K., Robertson, J. W., Turner, G. W., Vesper, D. N. 1994, in *Interacting Binary Stars*, ASP Conf. Ser. 56, ed. A. W. Shafter (San Francisco: Astronomical Society of the Pacific), 277
- Honeycutt, R. K., Turner, G. W. 1992, in *Robotic Telescopes in the 1990's*, ed. A. Filippenko (San Francisco: Astronomical Society of the Pacific), 77
- Humason, M. 1938, *ApJ*, 88, 228
- Jahoda, K., et al. 1996, in *EUV, X-Ray, and Gamma-Ray Instrumentation for Astronomy VII*, eds. O. H. Siegmund, M. A. Gummin, Proc. SPIE 2808, 59
- Kukarkin, B. V., et al. 1971, *General Catalogue of Variable Stars*, 3rd ed., 0
- Livio, M. 1989, in *Physics of Classical Novae*, Proc. IAU Colloq. 122, eds. A. Cassatella, R. Viotti (Berlin: Springer-Verlag), 342
- Livio, M., Pringle, J. E. 1994, *ApJ*, 427, 956
- Massey, P., Strobel, K., Barnes, J. V., Anderson, E. 1988, *ApJ*, 328, 315
- Mineshige, S. 1993, *Ap&SS*, 210, 83
- Osaki, Y. 1996, *PASP*, 108, 39
- Pringle, J. E. 1981, *ARA&A*, 19, 137
- Richman, H. R. 1996, *ApJ*, 462, 404
- Richman, H. R., Applegate, J. H., Patterson, J. 1994, *PASP*, 106, 1075
- Ringwald, F. A., Naylor, T., Mukai, K. 1996, *MNRAS*, 281, 192
- Ritter H., Kolb U. 1998, *A&AS*, 129, 83
- Roberts, D. H., Lehár, J., Dreher, J. W. 1987, *AJ*, 93, 968
- Shara, M. M. 1989, *PASP*, 101, 5
- Shara, M. M., Potter, M., Shara, D. J. 1989, *PASP*, 101, 985
- Stellingwerf, R. F. 1978, *ApJ*, 224, 953
- Szkody, P., et al. 1999, *ApJ*, 521, 362
- Verbunt, F., Bunk, W. H., Ritter, H., Pfeffermann, E. 1997, *A&A*, 327, 602
- Warner, B. 1995, *Cataclysmic Variable Stars* (New York: Cambridge University Press)
- Weight, A., Evans, A., Naylor, T., Wood, J. H., Bode, M. F. 1994, *MNRAS*, 266, 761
- Whitehurst, R. 1988, *MNRAS*, 232, 35
- Williams, G. 1983, *ApJS*, 53, 523

TABLE 1
LOG OF OBSERVATIONS FOR DI LAC

UT Date and Time ^a	HJD ^a	Observatory	Mode ^b	Exposure or GTI (s)	Comment
1990 Nov 12	2448207.7	RoboScope	P	240 ^c	starting date
1997 Jul 25 10:43:44	2450654.94822	RXTE	X	2528	ID 20037-02-01-00
1997 Jul 27 09:01:47	2450654.87744	APO	S	900	...
1997 Jul 27 09:16:53	2450654.88792	APO	S	737	...
1997 Jul 30 04:16:00	2450659.67921	RXTE	X	944	ID 20037-02-02-00
1997 Aug 03 04:11:12	2450663.68424	RXTE	X	1536	ID 20037-02-03-00
1997 Aug 07 04:12:00	2450667.67683	RXTE	X	1680	ID 20037-02-04-00
1997 Aug 12 03:42:40	2450672.65668	RXTE	X	592	ID 20037-02-05-00
1997 Aug 17 03:42:18	2450677.65666	APO	S	900	...
1997 Aug 17 03:45:36	2450677.65893	RXTE	X	1024	ID 20037-02-06-00
1997 Aug 23 03:46:40	2450683.65991	RXTE	X	832	ID 20037-02-07-00
1997 Aug 27 03:46:56	2450687.66024	RXTE	X	736	ID 20037-02-08-00
1997 Sep 01 08:12:48	2450692.84503	RXTE	X	1616	ID 20037-02-09-00
1997 Sep 03 05:56:28	2450694.74974	WIYN	S	900	No flux calibration
1997 Sep 04 04:33:17	2450695.69269	WIYN	S	900	No flux calibration
1997 Sep 06 08:08:48	2450697.84239	RXTE	X	1776	ID 20037-02-10-00
1998 Nov 30	2451147.6	RoboScope	P	240 ^c	ending date

^a At mid-point of exposure or Good-Time-Interval (GTI)

^b P = ground-based photometry; S = ground-based spectroscopy; X = X-ray

^c 1–2 measurements night⁻¹

TABLE 2
LOG OF OBSERVATIONS FOR V841 OPH

UT Date and Time ^a	HJD ^a	Observatory	Mode ^b	Exposure or GTI (s)	Comment
1991 May 31	2448407.7	RoboScope	P	240 ^c	starting date
1997 Apr 30 16:10:57	2450569.17897	RXTE	X	1936	ID 20037-01-01-00
1997 May 05 12:50:25	2450574.03997	RXTE	X	1856	ID 20037-01-02-00
1997 May 07 06:30:32	2450575.77120	APO	S	600	...
1997 May 10 20:59:13	2450579.37966	RXTE	X	1936	ID 20037-01-03-00
1997 May 14 06:37:42	2450582.77618	APO	S	600	...
1997 May 15 21:12:33	2450584.38911	RXTE	X	1408	ID 20037-01-04-00
1997 May 17 09:35	2450585.899	WIYN	S	4500	3 combined spectra
1997 May 20 07:58:41	2450588.83795	RXTE	X	1792	ID 20037-01-05-00
1997 May 26 06:28:11	2450594.77523	RXTE	X	1872	ID 20037-01-06-00
1997 May 27 06:22:21	2450595.76552	APO	S	600	...
1997 May 30 05:06:57	2450598.71888	RXTE	X	1648	ID 20037-01-07-00
1997 Jun 04 22:57:37	2450604.46244	RXTE	X	832	ID 20037-01-08-00
1997 Jun 09 06:43:45	2450608.78613	RXTE	X	2160	ID 20037-01-09-00
1997 Jun 18 16:24:33	2450618.18935	RXTE	X	1376	ID 20037-01-11-00 ^d
1998 Sep 04	2451060.5	RoboScope	P	240 ^c	ending date

^a At mid-point of exposure or Good-Time-Interval (GTI)

^b P = ground-based photometry; S = ground-based spectroscopy; X = X-ray

^c 1–2 measurements night⁻¹

^d Our tenth RXTE observation of V841 Oph on 1997 Jun 14 UT (ID 20037-01-10-00) was unusable due to a software event that shut down all of the detectors during the slew to the target.

TABLE 3
PERIODS IN OPTICAL LIGHT CURVES

Observing Season	DI Lac Period (d)	V841 Oph Period (d)
1	40	35
2	29	36
3	39	69
4	31	40
5	38	42
6	75,40	49
7	80,28	54
8	31,21	48
combined	43,37	49,36

TABLE 4
X-RAY SPECTRUM MODELS FOR DI LAC

Model	Reduced χ^2 (47 dof) ^a	P_0 ^b	H Column Density, N_{H} (10^{22} cm^{-2})	2–15 keV Model Flux ($\text{erg s}^{-1} \text{ cm}^{-2}$)	kT (keV)	Parameters ^c C_{norm}
Blackbody	0.705	0.937	≤ 1.2	2.2×10^{-12}	$1.1^{+0.1}_{-0.2}$	$3.0^{+0.6}_{-0.2} \times 10^{-5}$
Raymond-Smith ^d	0.617	0.982	≤ 3.3	2.6×10^{-12}	$3.2^{+0.7}_{-1.1}$	$3.4^{+3.5}_{-0.6} \times 10^{-3}$
Bremsstrahlung	0.484	0.999	≤ 1.8	2.7×10^{-12}	$4.5^{+1.3}_{-1.3}$	$1.1^{+0.7}_{-1.1} \times 10^{-3}$
H Column Density fixed from $E(B - V) = 0.15$:						
Blackbody	0.683	0.954	0.09	2.2×10^{-12}	$1.1^{+0.1}_{-0.1}$	$3.1^{+0.4}_{-0.3} \times 10^{-5}$
Raymond-Smith ^d	0.604	0.986	0.09	2.7×10^{-12}	$2.9^{+0.9}_{-0.5}$	$3.7^{+0.9}_{-0.9} \times 10^{-3}$
Bremsstrahlung	0.471	0.999	0.09	2.7×10^{-12}	$4.2^{+1.5}_{-1.0}$	$1.2^{+0.4}_{-0.3} \times 10^{-3}$
H Column Density fixed from $E(B - V) = 0.41$:						
Blackbody	0.689	0.951	0.24	2.3×10^{-12}	$1.1^{+0.1}_{-0.1}$	$3.3^{+0.3}_{-0.4} \times 10^{-5}$
Raymond-Smith ^d	0.606	0.986	0.24	2.7×10^{-12}	$2.9^{+0.9}_{-0.5}$	$3.8^{+0.9}_{-0.9} \times 10^{-3}$
Bremsstrahlung	0.475	0.999	0.24	2.7×10^{-12}	$4.1^{+1.4}_{-1.0}$	$1.2^{+0.4}_{-0.3} \times 10^{-3}$

^a 48 dof for fixed N_{H} models.

^b Null Hypothesis Probability: the probability of obtaining a value of χ^2 greater than or equal to the observed χ^2 if the model is correct. A value close to 1.0 indicates a good fit.

^c Quoted uncertainties are 1-parameter 90% confidence intervals. T is the plasma temperature for the bremsstrahlung and Raymond-Smith plasma models. In all models, C_{norm} is a normalization constant.

^d Additional model parameters of redshift and abundances were fixed at 0.0 and the values from Feldman (1992), respectively.